Article

Comparison of Energy Consumption and CO$_2$ Emission for Three Steel Production Routes—Integrated Steel Plant Equipped with Blast Furnace, Oxygen Blast Furnace or COREX

Jiayuan Song [1], Zeyi Jiang [1,*], Cheng Bao [1] and Anjun Xu [2]

[1] School of Energy and Environmental Engineering, University of Science and Technology Beijing, Beijing 100083, China; songjiayuan2015@outlook.com (J.S.); baocheng@mail.tsinghua.edu.cn (C.B.)

[2] School of Metallurgical and Ecological Engineering, University of Science and Technology Beijing, Beijing 100083, China; anjunxu@metall.ustb.edu.cn

* Correspondence: zyjiang@ustb.edu.cn; Tel.: +86-10-6233-2741; Fax: +86-10-6233-2741

check for updates

Abstract: High CO$_2$ emissions and energy consumption have greatly restricted the development of China's iron and steel industry. Two alternative ironmaking processes, top gas recycling-oxygen blast furnace (TGR-OBF) and COREX$^®$, can reduce CO$_2$ emissions and coking coal consumption in the steel industry when compared with a conventional blast furnace (BF). To obtain parameters on the material flow of these processes, two static process models for TGR-OBF and COREX were established. Combining the operating data from the Jingtang steel plant with established static process models, this research presents a detailed analysis of the material flows, metallurgical gas generation and consumption, electricity consumption and generation, comprehensive energy consumption, and CO$_2$ emissions of three integrated steel plants (ISP) equipped with the BF, TGR-OBF, and COREX, respectively. The results indicated that the energy consumption of an ISP with the TGR-OBF was 16% and 16.5% lower than that of a conventional ISP and an ISP with the COREX. Compared with a conventional ISP, the coking coal consumption in an ISP with the TGR-OBF and an ISP with the COREX were reduced by 39.7% and 100% respectively. With the International Energy Agency factor, the ISP with the TGR-OBF had the lowest net CO$_2$ emissions, which were 10.8% and 35.0% lower than that of a conventional ISP and an ISP with the COREX. With the China Grid factor, the conventional ISP had the lowest net CO$_2$ emissions—2.8% and 24.1% lower than that of an ISP with the TGR-OBF and an ISP with the COREX, respectively.

Keywords: oxygen blast furnace; COREX; static process model; integrated steel plant; material flow; energy consumption; CO$_2$ emissions

1. Introduction

Steel is the world's most popular construction material due to its durability, processability, and cost. However, producing steel creates high energy consumption and CO$_2$ emissions. According to the World Steel Association, the production of crude steel reached 1691 million tons in 2017 and the large amount of crude steel production resulted in about 3.1×10^{11} GJ of energy consumption and 3043.8 million tons of CO$_2$ emissions [1]. The blast furnace (BF)—basic oxygen furnace (BOF) route is the dominant steel production route in the world, and its ironmaking process contributes approximately 70% of the above energy consumption and CO$_2$ emissions [2]. Many studies have shown that adopting commercially available energy-saving technologies for BF has significantly reduced the energy consumption of the ironmaking process [3] and almost reached the thermodynamic limits of

BF [4]. Thus, in order to minimize the energy consumption and CO_2 emissions of the ironmaking process, alternative liquid iron production technologies to BF such as top gas recycling-oxygen blast furnace (TGR-OBF) and COREX have been proposed and developed.

The oxygen blast furnace (OBF) is a type of metallurgical furnace used for producing liquid iron, which was proposed by Wenzel and Gudenau in 1970 [5]. However, the first generation of OBF had the problem of overheating in the lower part of the furnace and thermal shortage in the upper part of the furnace. In order to solve these problems, some TGR-OBF processes such as Fink [6], Lu [7], Nippon Kokan Steel (NKK) [8], Tula [9], full oxygen blast furnace (FOBF) [10], and Ultra-Low CO_2 Steelmaking initiative (ULCOS) [11] have been proposed. In the TGR-OBF process, iron ore, coke, and flux are supplied through the top of OBF in succession, while normal temperature oxygen and pulverized coal are injected into the OBF by tuyeres at the bottom. The preheated top gas is recycled into the OBF at the lower stack, after the removal of CO_2 and H_2O. Compared with the BF process, the two key characteristics of the TGR-OBF process are the injection of pure oxygen as an oxidant instead of a hot blast and the recycling of top gas as a reductant after the removal of CO_2 and H_2O and preheating. These characteristics increase the amount of pulverized coal in the OBF to more than 300 kg/t-hot metal [12] and reduced the coke ratio to less than 200 kg/t-hot metal [13]. As a result of the study of a pilot plant, an 8 m^3 experimental TGR-OBF built during the Ultra-low CO_2 steelmaking initiative phase I (ULCOS I) showed that the TGR-OBF process was feasible and could significantly reduce the consumption of coke and CO_2 emissions in the ironmaking process [14]. Moreover, many researchers have conducted experiments and numerical simulations of the TGR-OBF process, which showed that the TGR-OBF process is a promising alternative liquid iron production technology given its low coke consumption and CO_2 emissions [15–18].

COREX is an industrially and commercially proven smelting reduction ironmaking process and was created by Siemens Voest-Alpine Industrieanlagenbau Gmbh & Co. (VAI) in the 1970s [19]. There are eight COREXs in the world that have been successfully commercialized [20]; two of which are the latest generation of COREX with a capacity of 1.5 million tons of liquid iron per year and were built in China at the Baosteel Luojing steel plant [21]. The characteristic of COREX is the separation of the iron reduction and smelting operations into two separate reactors, namely the upper reduction shaft and the lower melter-gasifier [22]. In the upper reduction shaft, iron ore and flux are continuously charged from the top of the shaft. They descend by gravity and are reduced into approximately 95% direct reduced iron by the reduction gas generated from the melter-gasifier. In the melter-gasifier, the reduction shaft products—direct reduced iron—is fed from the top of the melter-gasifier for further reduction and melting. Non-coking coal and room temperature oxygen, as the main reductant and oxidant, are injected via the lock hopper system at the top of the melter-gasifier and tuyeres at the bottom of the melter-gasifier, respectively. After being purified by hot gas cyclones, a major part of the top gas from the melter-gasifier is cooled and subsequently added to the reduction shaft. The excess gas and the reduction shaft gas are mixed before the take-over point, called the COREX export gas. When compared with the BF or TGR-OBF process, the COREX process can directly produce liquid iron without using coking coal, sinter, or pellets. The COREX process combines the coking plant, sinter plant, and blast furnace or oxygen blast furnace into a single ironmaking process. Therefore, as an alternative liquid iron production technology to BF, further research into the TGR-OBF and COREX steel production processes are of great significance.

Most of the studies on TGR-OBF and COREX have focused on a reaction unit rather than the ISP. Wenlong et al. estimated the impact of different metallization rates and fuel structures on the energy consumption of the COREX process by using a modified Rist operating diagram [23]. Hu et al. compared the CO_2 emissions between the COREX and blast furnace ironmaking system based on carbon element flow analysis [24]. Lianzhi et al. used a two-dimensional numerical simulation model to analyze the effect of top gas recycling on the blast furnace status, productivity, and energy consumption. The results showed that TGR-OBF productivity increased by 5.3–35.3% and the energy saving was 27.3–35.9% when compared to blast furnaces [17]. Wei et al. conducted exergy analyses

of the TGR-OBF ironmaking process [18]. Xuefeng et al. investigated the carbon saving potential of the TGR-OBF ironmaking process from the perspective of the relationship between the degree of direct reduction and carbon consumption [25]. These studies demonstrated well the effect of operating parameters on energy consumption and CO_2 emissions in the COREX or TGR-OBF process. However, focusing only on a specific unit like the ironmaking process will make it difficult for policymakers to fully understand the alternative ironmaking process from a mill-wide perspective. Up to now, many studies conducted from a plant-wide perspective are based on only the one steel production route. Hooey et al. made a techno-economic comparison of an ISP equipped with the OBF and CO_2 capture by using process and economic models and found that the OBF with CO_2 capture offered a significant potential to reduce the overall CO_2 emissions from an ISP, achieving 47% CO_2 avoidance at a cost of ~$56/t CO_2 for the given assumptions [26]. Huachun et al. analyzed the energy consumption and carbon emissions of a conventional ISP by using an integrated material flow analysis model [27]. Jin et al. analyzed the energy consumption and carbon emissions of an ISP with the TGR-OBF route, according to an established heat transfer and reaction kinetics mathematical model for the TGR-OBF ironmaking process. The results indicate that the energy consumption of an ISP with the TGR-OBF route was reduced to 14.4 GJ per ton of crude steel; moreover, the direct CO_2 emissions were reduced by 26.2% per ton of crude steel when compared with a conventional ISP [28]. Arasto et al. analyzed the technical assessment of the application of OBF with CCS to an ISP. The analysis showed that the CO_2 emissions from an ISP could be significantly reduced by the application of an oxygen blast furnace and CCS [29]. Based on the technical analysis, the economic profitability was further evaluated in Reference [30], which found that the investment on OBF or CCS depended on CO_2, the fuels, and electricity prices. However, the comprehensive energy consumption and CO_2 emissions analysis on three different routes based on the static process model such as an ISP with BF, an ISP with the TGR-OBF, and an ISP with the COREX were not analyzed in detail.

Therefore, in this study, TGR-OBF and COREX static process models were developed based on the mass and heat balance to obtain the material and energy flow parameters of the two ironmaking processes. Combining the operating data from the Jingtang steel plant with established static process models, this research presents a detailed analysis on the material flow, metallurgical gas generation and consumption, electricity consumption and generation, comprehensive energy consumption, and CO_2 emissions of the BF, TGR-OBF, and COREX in an ISP.

2. Models and Methods

2.1. Static Process Models

The objective of this study is to compare different steel production routes under the same composition and temperature of the hot metal, as well as the same chemical composition of raw materials (For the TGR-OBF, the raw materials with the same composition as the BF are flux, coke, coal, sinter, and pellets. For the COREX, the raw materials with the same composition as the BF are flux, and coal). Thus, on the basis of the mass and heat balance principles, a TGR-OBF static process model based on our previous research—References [17,28,31] and a COREX static process model based on the Baosteel COREX3000 were established by using the gPROMS Modelbuilder platform. According to the calculation of the two static process models, the consumption of raw material and fluxes, the production and composition of slag and metallurgical gas per ton of hot metal can be obtained. Combining the two static process models with the ISP of the Jingtang, this research presents a detailed comparison and analysis of the three ISPs equipped with the BF, TGR-OBF, and COREX, respectively.

2.1.1. The TGR-OBF Process Model

The flow diagram of the TGR-OBF process is shown in Figure 1. In the TGR-OBF process, most of the top gas is recycled into the furnace as the recycled gas after CO_2 removal and preheating. Part of the recycled gas is injected at the hearth tuyeres, another part of the recycled gas is injected at the

lower shaft. This kind of gas recycling in the TGR-OBF process could effectively supplement the heat and reducing atmosphere in the shaft area, and also reduced the combustion temperature in the tuyere area [17]. In this study, the total amount of the recycled gas assumed was 600 m^3/t-HM, the upper and lower recycled gas assumed were 300 m^3/t-HM, respectively (Supplementary Materials Table S7). This condition could ensure the successful operation of the TGR-OBF and provide high calorific value gas for other processes, as well as ensure the balance of the metallurgical gas in the ISP [31]. Moreover, based on our previous research [31], the temperature of the recycled gas at the hearth tuyeres had little effect on the burn-out rate of the pulverized coal (when the temperature of the recycled gas raised from 298 K to 1500 K, the burnout rate of the pulverized coal only changed by 1.5%). Therefore, considering the technical difficulty and the cost, the recycled gas was assumed to be preheated to 1173 K (Table S7). The main reactions in the furnace include the reduction of various iron oxides by CO/H_2, the decomposition of carbonate, coke, and coal, and the combustion of carbon and reducing gas. In order to make the TGR-OBF process operate successfully under the certain conditions of the raw materials and fuel, it is very important to select reasonable slag-forming practices to make the slag have a better performance. The performance of the slag is closely related to its chemical composition. The basicity is an important parameter of measuring the viscosity of the slag, at the same time, the basicity has great influence on the melting and stability of the slag. Therefore, the binary basicity R_2 (Equation (3)) of the slag were included as the constrained equation. Based on the following balance Equations (1), (3), and (4) in the TGR-OBF process, the consumption of raw materials (sinter, pellets, limestone, and dolomite), the amount and chemical composition of slag can be obtained by giving the value of chemical composition of raw materials and hot metal (Tables S1, S2, S4, and S6).

- Mass balance:

$$\sum_{in} m_i \times \omega(x)_i = \sum_{out} m_j \times \omega(x)_j. \tag{1}$$

When the consumption of raw materials was calculated, the mass balance equations included the Fe balance equation, the S balance equation, the CaO balance equation, the SiO_2 balance equation, the Al_2O_3 balance equation, the MgO balance equation, the MnO balance equation, and the P_2O_5 balance equation. Taking the Fe balance equation as an example,

$$\sum_i m_i \times \omega(Fe)_i = m_{HM} \times \omega(Fe)_{HM} + m_{slag} \times \omega(FeO)_{slag} \times 56/72 \tag{2}$$

- Binary basicity:

$$R_2 = m_{\text{CaO-slag}} / m_{\text{SiO}_2\text{-slag}} \tag{3}$$

- Quantity of slag:

$$m_{\text{slag}} = m_{\text{FeO-slag}} + m_{\text{CaS-slag}} + m_{\text{CaO-slag}} + m_{\text{SiO}_2\text{-slag}} + m_{\text{Al}_2\text{O}_3\text{-slag}} + m_{\text{MgO-slag}} + m_{\text{MnO-slag}} + m_{\text{P}_2\text{O}_5\text{-slag}} \tag{4}$$

where m_i is the mass of sinter, pellets, coke, coal, limestone, and dolomite for producing 1 ton of hot metal, kg; $\omega(Fe)_i$ is the mass fraction of Fe in material i; $\omega(FeO)_{slag}$ is the mass fraction of FeO in slag; m_{HM} is the mass of hot metal, which in this study was 1 ton; m_{slag} is the mass of slag, kg; and $\omega(x)_i$ is the composition of x in material i, %.

The utilization of hydrogen in the top gas and the oxidation degree of the top gas are important parameters that can affect the chemical composition of the top gas. Therefore, the utilization of hydrogen in the top gas and the oxidation degree of the top gas were included as the constrained equations. Based on the operating conditions and parameters (Tables S3 and S7) of the TGR-OBF process, the volume and chemical composition of top gas were obtained by calculating the following balance Equations (5)–(9), and (11).

- C balance:

$$\sum_i m_i \times \omega(C)_i + V_{rg} \times [v(CO)_{rg} + v(CO_2)_{rg}] \times 12/22.4 = (V_{CO} + V_{CO_2} + V_{CH_4}) \times 12/22.4 + m_{HM} \times \omega(C)_{HM} + m_{dust} \times \omega(C)_{dust} \quad (5)$$

- H balance:

$$\sum_i m_i \times \omega(H)_i + V_{rg} \times [v(H_2)_{rg} + v(H_2O)_{rg}] \times 2/22.4 = (4 \times V_{CH_4} + 2 \times V_{H_2} + 2 \times V_{H_2O})/22.4 \quad (6)$$

- N balance:

$$\sum_i m_i \times \omega(N)_i + V_{rg} \times v(N_2)_{rg} \times 28/22.4 = V_{N_2} \times 28/22.4 \quad (7)$$

- The utilization of hydrogen in the top gas:

$$\eta_{H_2} = V_{H_2O_r}/V_{H_2O_r} + V_{H_2} \quad (8)$$

- The oxidation degree of the top gas:

$$OD = (V_{H_2O} + V_{CO_2})/(V_{H_2O} + V_{CO_2} + V_{H_2} + V_{CO}) \quad (9)$$

here, V_{rg} is the volume of recycled gas; V_{CO}, V_{H2O}, V_{CO2}, V_{H2}, V_{CH4}, and V_{N2} are the volume of CO, H_2O, CO_2, H_2, CH_4, and N_2 in top gas for producing 1 ton of hot metal, m³, respectively; V_{H2Or} is the volume of water in the top gas, which was produced by the reduction, m³; $v(CO)_{rg}$, $v(CO_2)_{rg}$, $v(H_2)_{rg}$, $v(H_2O)_{rg}$, $v(N_2)_{rg}$ are the volume fraction of CO, CO_2, H_2, H_2O, and N_2 in recycled gas, respectively; $\omega(C)_i$, $\omega(H)_i$, $\omega(N)_I$ and $\omega(C)_{HM}$ are the mass fraction of C, H, and N in material i and hot metal, respectively; and T_{gas} is the temperature of the metallurgical gas, K.

- Heat balance:

$$\sum_{in} m_i w_i(x) \cdot h_i + \sum_{in} m_i \cdot q_i = \sum_{out} m_j w_j(x) \cdot h_j + \sum_{out} m_j \cdot q_j + H_l \quad (10)$$

where h_i, h_j are the enthalpy of the chemical reaction, kJ/kg; q_i, q_j are the sensible heat, kJ/kg; and H_l is the enthalpy of loss, kJ.

Based on the above calculation results and the oxygen balance equation of the furnace, the volume of oxygen blast can be obtained. Based on the mass balance of the gas in top, bosh, and hearth of the furnace, and the heat balance (Equation (10)) of the whole furnace, the volume of recycled gas can be obtained. The volume of gas required for preheating the recycled gas is obtained by the heat balance (Equation (10)) of the heater unit. The parameters calculated by the TGR-OBF static process model are shown in Tables S1–S7 (Supplementary Materials).

In the VPSA unit, the recovery rate of CO_2 was set at 90% [32], and the energy consumption was set at 645.7 kJ/kg-CO_2 [33]. In the heater unit, the thermal efficiency was set at 86% [11].
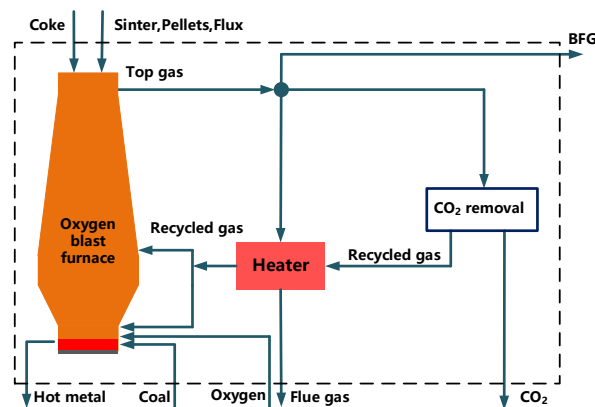

Figure 1. The flow diagram of top gas recycling-oxygen blast furnace (TGR-OBF) ironmaking process.

2.1.2. The COREX Process Model

The COREX process flow chart is shown in Figure 2. The COREX process is comprised of the shaft furnace and melter-gasifier. In the shaft furnace, the main reactions include the reduction of various iron oxides and carbonate decomposition, while the main reactions inside the melter-gasifier include coal decomposition, carbon and reducing gas combustion, reduction of residual iron oxides, and decomposition of residual carbonate. In the COREX process, the raw gas produced by the melter-gasifier is first purified by hot gas cyclones. The dust after cyclone removal is recycled back to the melter-gasifier by dust burners. The major part of the purified raw gas is made available as reduction gas for the reduction shaft. Additionally, the rest of the purified top gas is scrubbed and mixed with the cleaned reduction shaft top gas to form COREX gas. The static process model and its operating parameters are based on Baosteel COREX 3000.

Based on the Tables S1, S2, S4, and S6, the consumption of raw materials (iron ore, limestone, and dolomite), the amount and chemical composition of slag can be calculated by using balance Equations (1), (3), and (4) in the COREX process. Based on the operating conditions and parameters (supplementary materials Tables S3 and S10) and the equation 11 of the COREX process, the volume and chemical composition of raw gas can be obtained by calculating balance Equations (9), and (11)–(14).

- H balance:

$$\sum_i m_i \times \omega(\mathrm{H})_i = (4 \times V_{\mathrm{CH_4}} + 2 \times V_{\mathrm{H_2}} + 2 \times V_{\mathrm{H_2O}})/22.4 \tag{11}$$

- C balance:

$$\sum_i m_i \times \omega(\mathrm{C})_i = (V_{\mathrm{CO}} + V_{\mathrm{CO_2}} + V_{\mathrm{CH_4}}) \times 12/22.4 + m_{\mathrm{HM}} \times \omega(\mathrm{C})_{\mathrm{HM}} \tag{12}$$

- N balance:

$$\sum_i m_i \times \omega(\mathrm{N})_i = V_{\mathrm{N_2}} \times 28/22.4 \tag{13}$$

- The equilibrium constant of the water gas shift reaction:

$$K = (V_{\mathrm{CO_2}} + V_{\mathrm{H_2}})/(V_{\mathrm{H_2O}} + V_{\mathrm{CO}}) = \exp[(29,490 - 26.8 \times T_{\mathrm{gas}})/(8.314 \times T_{\mathrm{gas}})] \tag{14}$$

where, V_{CO}, V_{H2O}, V_{CO2}, V_{H2}, V_{CH4}, and V_{N2} are the volume of CO, H_2O, CO_2, H_2, CH_4, and N_2 in top gas for producing 1 ton hot metal, m³; $\omega(\mathrm{C})_i$, $\omega(\mathrm{H})_i$, $\omega(\mathrm{N})_i$ and $\omega(\mathrm{C})_{\mathrm{HM}}$ are the mass fraction of C, H, N in material i and hot metal, respectively; T_{gas} is the temperature of the raw gas, K.
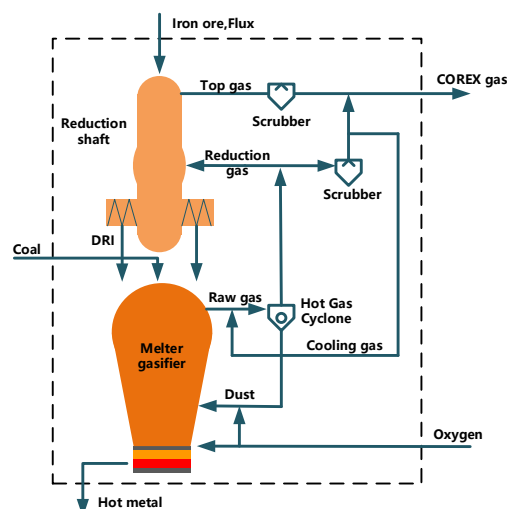

Figure 2. The flow diagram of the COREX® ironmaking process.

Based on the volume, temperature, and composition of the raw gas, the volume of the cooling gas can be calculated by the heat balance (Equation (10)) of the hot gas cyclone. The consumption of coal is obtained by the heat balance (Equation (10)) of the melter-gasifier. The oxygen consumption can be obtained by the oxygen balance of the melter-gasifier. The volume of top gas can be obtained by the mass balance of the shaft furnace and gas oxidation degree. Finally, based on the mass balance of the metallurgical gas, the volume of COREX gas can be obtained. The parameters of the COREX process calculated by the COREX static process model are shown in Tables S1–S4, S6, and S9 (Supplementary Materials).

2.2. Integrated Steel Plant

As shown in Figure 3, the ISP consists of the steel manufacturing system and the energy system. The steel manufacturing system is comprised of the raw material handling process, ironmaking process, steelmaking process, and steel rolling process. In the steel manufacturing system, the iron ore is made into steel production with the help of energy inputs. At the same time, the generated metallurgical gases (including coke oven gas, blast furnace gas, and Linz-Donawitz gas), generated electricity, generated oxygen, and steam are controlled by the energy system. As a buffer, the power plant and oxygen plant can convert the surplus metallurgical gas from the steelmaking system into electricity and oxygen. For the BF and TGR-OBF steelmaking routes, the raw material handling processes include coking, sintering, and pelletizing, while the COREX steel production route does not. The analysis scale of an ISP was based on 1 t crude steel. In the analysis of a conventional ISP, the conventional ISP of Jingtang (which is located in the north of China) was taken as a reference case. By calculating the static process models of the TGR-OBF process and COREX process, the input and output parameters of per ton of hot metal in the two ironmaking processes can be obtained. On the basis of the hot metal consumption per ton of crude steel in the jingtang steel plant, combining the two static process models with the operation data of Jingtang steel plant (without BF process), an ISP with the TGR-OBF and an ISP with the COREX can be analyzed. In the analysis of the three ISPs, the following assumptions were made in this study:

1. In the calculation of the TGR-OBF and COREX process models, the temperature and composition of hot metal, the chemical composition of raw materials were considered to be the same as that of the BF process in the Jingtang steel plant, and it was feasible for the two ironmaking processes. For the TGR-OBF process, the raw materials with the same composition as the BF were flux, coke, coal, sinter, and pellets. For the COREX process, the raw materials with the same composition as the BF were flux and coal.

2. For a better comparison of the three ironmaking technology in the ISP, the static process model of the TGR-OBF established in this paper was based on the current feasible technology, and the CCS technology was not considered in this study.

3. In the analysis of an ISP with the TGR-OBF and an ISP with the COREX, the operation data for the raw materials handling process, steelmaking process, rolling process, lime making process, oxygen plant, and power plant were all from the Jingtang steel plant. The input and output values of the raw materials handling process were proportional to the raw material consumption of the TGR-OBF process and COREX process, respectively.

4. In an ISP, the metallurgical gas was preferentially supplied to the steel manufacturing system for use. The surplus gas was transported to the power plant, and the generating efficiency was 33%.

5. The blast furnace blower was driven by electricity and the power consumption was 0.103 kWh/m³.

6. Since the calculation of TRT power generation is very complex. In this study, the generating capacity was simplified to be only related to the flow of top gas, it was 0.028 kWh/m³.

7. The electricity consumption of cryogenic oxygen process is 0.86 kWh/m³-oxygen.

Therefore, based on the same composition and temperature of the hot metal, without changing the raw materials composition, the comparison and analysis of the three steel production routes can be obtained.
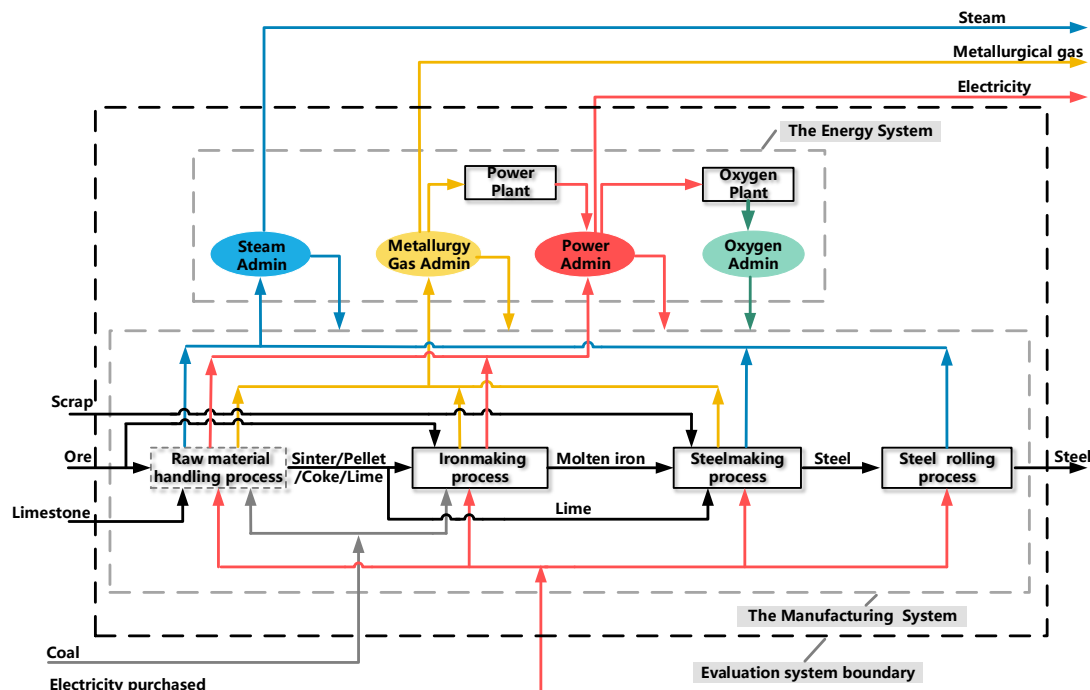

Figure 3. The integrated steel plant (ISP) in this study.

2.3. Methods to Calculate Comprehensive Energy Consumption

The calculation of comprehensive energy consumption of per ton steel is based on the energy balance of an ISP by using the energy equivalent value of each energy substance [34]. In a conventional ISP or an ISP with TGR-OBF, the energy substances input into the system mainly include injection coal, coking coal, and electricity, and the outputs mainly include electricity, chemical by-products, and steam. In an ISP with COREX, the energy substance input into the system mainly includes coal and electricity, and the output mainly includes electricity and steam. The equation of comprehensive energy consumption of per ton steel is as follows:

$$E = \sum_{i=1}^{m}\left(e_i^{in} \times p_i\right) - \sum_{i=1}^{n}(e_i^{out} \times p_i) \tag{15}$$

where e_i^{in}, e_i^{out} are the input and output energy substances i (kg/t crude steel); p_i is the energy conversion coefficient of substance i (GJ/kg); and m, n are the number of energy substances.

2.4. Methods to Calculate CO_2 Emissions

As proposed in the WRI & WBCSD (World Resources Institute & World Business Council for Sustainable Development) guidelines, the net CO_2 emissions are calculated by the direct CO_2 emissions, the indirect CO_2 emissions and the CO_2 credit [35]. In an ISP, the combustion of fossil fuel, metallurgical gas, and the decomposition of carbonate contribute to the direct CO_2 emissions, the purchased electricity and steam contribute to the indirect CO_2 emissions, and the excess steam, electricity, and chemical by-products can be considered as CO_2 credit. The net CO_2 emissions can be calculated by the following equations,

$$CE = CE_d + CE_i - CE_c \tag{16}$$

$$CE_d = (C_{in} - C_p - C_{byp})/12 \times 44 \tag{17}$$

where CE, CE_d, CE_i, CE_c represent the net, direct, indirect, and credit of the CO_2 emissions, t/t crude steel, respectively; and C_{in}, C_p, C_{byp} represent the amount of total carbon input to the system, the amount of carbon fixed in the product, and the amount of carbon fixed in the byproduct, t/t crude steel.

3. Results and Discussion

3.1. Material Flows Analysis

Based on the operating data of the Jingtang steel plant, the material flows of a conventional ISP were investigated and presented in Figure 4. For a better comparison with a conventional ISP, the material flows of an ISP with the TGR-OBF and an ISP with the COREX were studied by combining the operating data in the Jingtang steel plant with established static process models, as shown in Figures 5 and 6. The parameters of the TGR-OBF process and the COREX process analyzed in the ISP are shown in Figures S1 and S2 (Supplementary Materials). As shown in Figure 4, a large amount of coking coal was consumed by a conventional ISP with 487.4 kg/t-crude steel, and the consumptions of coal and oxygen were 134.3 kg/t-crude steel and 96.9 m³/t-crude steel, respectively. In a conventional ISP, the total production of blast furnace gas (BFG) and coke oven gas (COG) were 1336.3 m³/t-crude steel and 166.8 m³/t-crude steel. Most were used to maintain production for each main process, and the surplus BFG and COG were transferred to the power plant for power supply and network pressure maintenance. As Figures 5 and 6 demonstrate, the material flows of an ISP with the TGR-OBF and an ISP with the COREX changed significantly in comparison with a conventional ISP. Compared with a conventional ISP, the coking coal consumption in the ISP with the TGR-OBF reduced by 39.7%. Since coking coal is not used in the production process of the COREX, the amount of coking coal was zero. However, the coal consumption in the ISP with the TGR-OBF and the ISP with the COREX increased by 23.6% and 535.2%, respectively. This is because the top gas recycling in the TGR-OBF reduced the coke consumption and oxygen blast increased the coal consumption. In the ISP with the COREX, there was no coking process and the consumption of coal and oxygen greatly increased in the melter-gasifier. At the same time, oxygen consumption increased by 174.7% and 521.5% in the TGR-OBF and COREX, respectively. In addition, due to the reduction in coke consumption and top gas recycling, the metallurgical gas produced in the ISP with the TGR-OBF was significantly reduced in comparison with the conventional ISP, i.e., the BFG and COG were reduced by 84% and 39.7%, respectively. In this steel production route, almost no surplus metallurgical gas was transported to the power plant for power generation. However, in the ISP with the COREX, a large amount of coal was used to make iron, so the generated COREX gas was very large, which was 23.9% more than the BFG process.
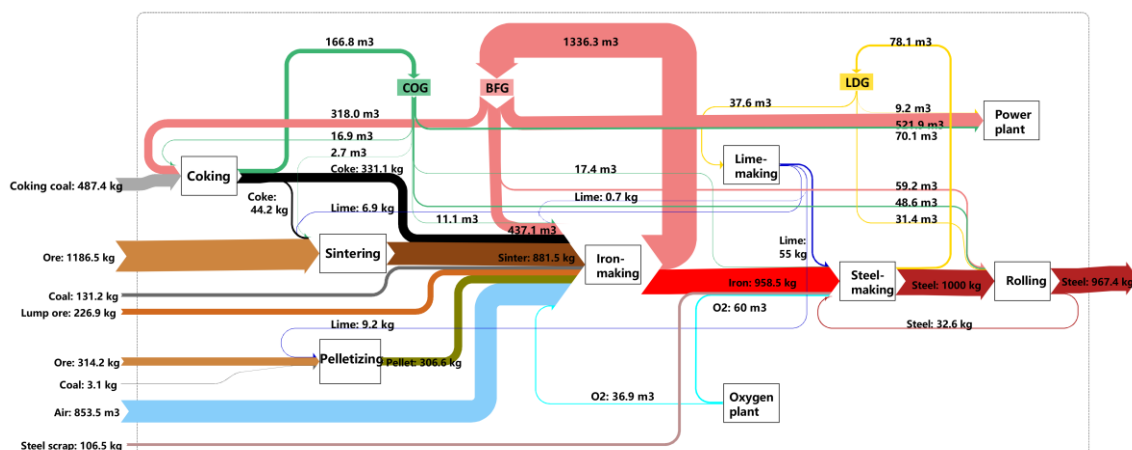

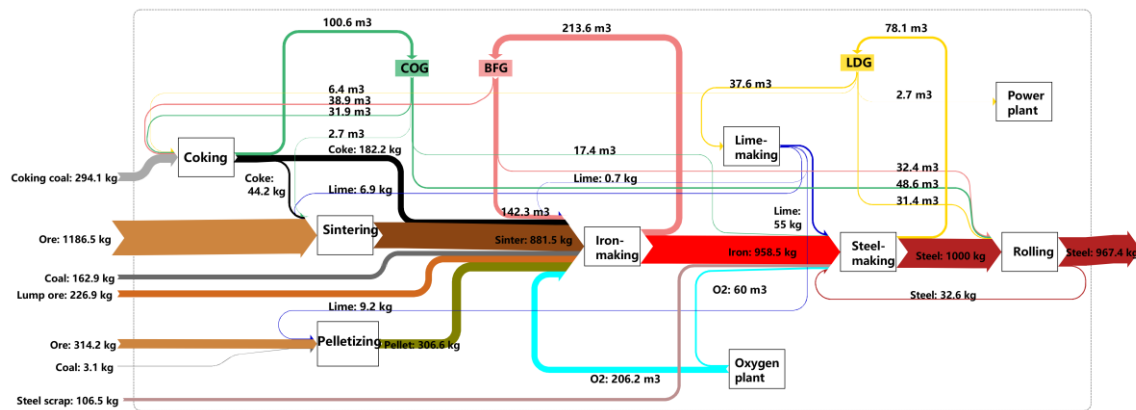**Figure 4.** Chart of the material flows of a conventional ISP.

Figure 5. Chart of the material flows of an ISP with the TGR-OBF.
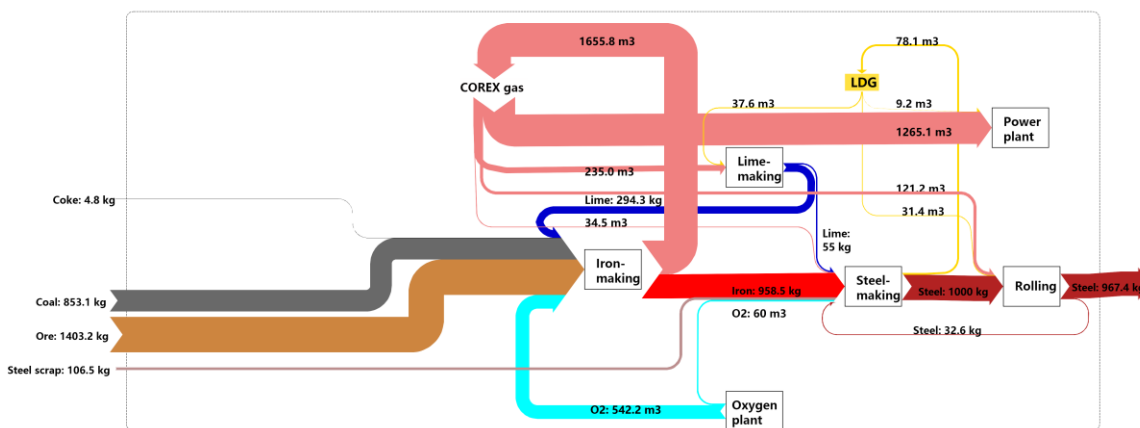

Figure 6. Chart of the material flows of an ISP with the COREX.

3.2. Metallurgical Gas Analysis

Figure 7 illustrates the generation and consumption of metallurgical gas by each process in a conventional ISP, an ISP with the TGR-OBF, and an ISP with the COREX. The order of metallurgical gas generation in the three ISPs is: ISP with the COREX (12.3 GJ/t-steel) > conventional ISP (7.8 GJ/t-steel) > ISP with the TGR-OBF (3.6 GJ/t-steel). This is because the oxygen consumption and coal consumption increased to 602.2 m³/t-crude steel and 853.1 kg/t-crude steel in an ISP with the COREX. The ISP with the TGR-OBF generated the least amount of metallurgical gas because of the use of recycled top gas. In addition, the ironmaking process of the ISP with the COREX contributed most of the metallurgical gas with 11.6 GJ/t-steel. This is because the ISP with COREX does not have a coking process, and a large amount of oxygen and coal react in the melter-gasifier to produce a large amount of high heat value COREX gas. In the coking process, the amount of COG in the conventional ISP and the ISP with the OBF were different. Compared with a conventional ISP (2.6 GJ/t-steel), the ISP with the TGR-OBF generated less COG with 1.6 GJ/t-steel. This is because the coke usage dropped to 294.1 kg/t-steel in the ironmaking process. The processes of metallurgical gas consumption included the power plant, ironmaking, coking, rolling, lime making, and steelmaking. In the ISP with COREX, 9.0 GJ/t-steel metallurgical gas was applied to the power plant, while only 2.9 GJ/t-steel and 0.027 GJ/t-steel were applied to power plants in a conventional ISP and an ISP with TGR-OBF.

Since an ISP with COREX does not include the coking process, sintering process, and pelletizing process, the amount of gas used in the steel manufacturing system is low and the amount of gas generated is large. Most of the surplus gas has to be sent to power plants for power generation.
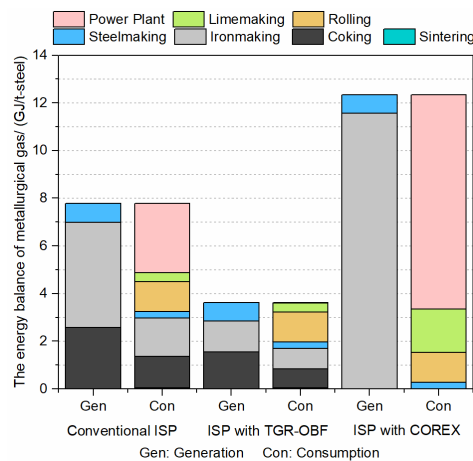
Figure 7. The metallurgical gas balance in the conventional ISP, ISP with the TGR-OBF, and ISP with the COREX.

3.3. Electricity Analysis

Figure 8 presents the generation and consumption of electricity by each process in a conventional ISP, an ISP with the TGR-OBF, and an ISP with the COREX. The electricity generated by the power plant was from the surplus metallurgical gas. Among the three steel production routes, the generation of electricity in an ISP with the COREX was the highest, followed by the conventional ISP, and the ISP with the TGR-OBF, which were 823.9 kWh/t-crude steel, 305.2 kWh/t-crude steel, and 35.4 kWh/t-crude steel, respectively. This is mainly because there is a large amount of surplus high heating value of metallurgical gas in an ISP with the COREX. The top gas recycling in an ISP with the TGR-OBF reduced the metallurgical gas production of the ironmaking and coking process, so almost no surplus metallurgical gas was transported to the power plant. Furthermore, the consumption of electricity in the ISP with the COREX was also the highest, followed by an ISP with the TGR-OBF, and the conventional ISP was the lowest. The increased demand for oxygen from the COREX and TGR-OBF was responsible for the significant increase in electricity consumption in the oxygen plant. As a result, the electricity consumed by the oxygen plant increased by 521.6% and 174.7%, respectively in comparison with the conventional ISP. Nevertheless, the ironmaking process of the ISP with the TGR-OBF consumed the most electricity in comparison with that of the other two steel production routes because the CO_2 removal unit in the TGR-OBF process raises the demand for electricity. When compared with a conventional ISP, the electricity consumption in the ironmaking process of the ISP with the TGR-OBF increased by 89%. Therefore, as presented in Figure 8, the ISP with TGR-OBF purchased the most electricity, followed by the conventional ISP, and the ISP with COREX purchased the least, which were 710.1 kWh/t-crude, 212.4 kWh/t-crude, and 77.3 kWh/t-crude, respectively.

3.4. Comprehensive Energy Consumption Analysis

The comprehensive energy consumptions of the conventional ISP, the ISP with the TGR-OBF, and the ISP with the COREX are shown in Figure 9. Among these three steel production routes, the ISP with the TGR-BOF consumed the least energy to produce 1 t of steel. The energy consumption was 14.16 GJ/t-steel, 16% and 16.5% lower than the conventional ISP and the ISP with the COREX, respectively. This is because the top gas recycling in the TGR-OBF ironmaking process can significantly reduce carbon consumption; despite requiring the most electricity to be purchased, the energy conversion coefficient of electricity is smaller than that of coal. Therefore, the comprehensive energy consumption in the ISP with the TGR-OBF is the lowest. Moreover, the energy consumed by the conventional ISP and the ISP with the COREX were 16.85 GJ/t-steel and 16.96 GJ/t-steel, respectively. However, the coking coal consumption accounted for 80.2% of the total energy input in the conventional ISP, which was the most out of the three steel production routes.
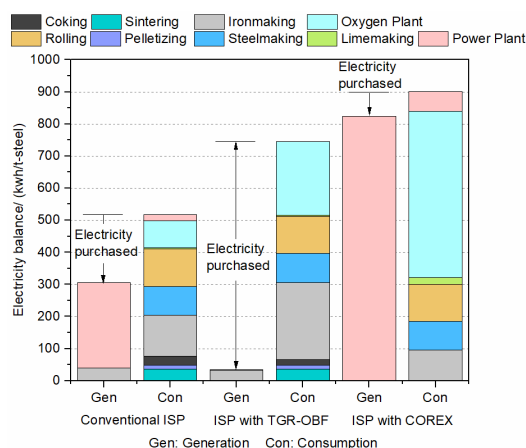
Figure 8. The electricity balance in the conventional ISP, the ISP with the TGR-OBF, and the ISP with the COREX.
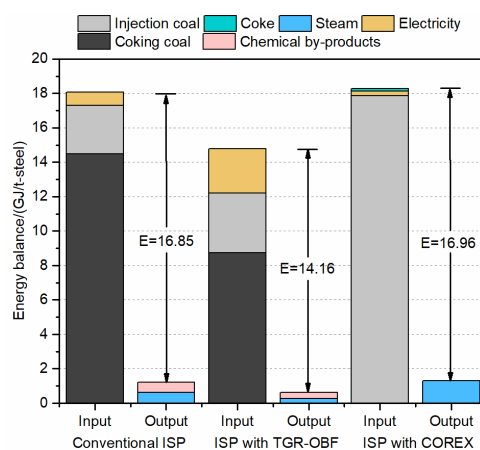

Figure 9. The energy balance in the conventional ISP, the ISP with the TGR-OBF, and the ISP with the COREX.

3.5. CO_2 Emissions Analysis

Figure 10 shows the net, direct, indirect, and the credit of CO_2 emissions in the three steel production routes with different CO_2 emissions factors. CCS technology was not considered in this research. When considering the impact of the CO_2 emissions factor of electricity, the International Energy Agency factor (0.504) and the China Grid factor (1.0302) were used to analyze the CO_2 emissions. In the conventional ISP, the ISP with the TGR-OBF, and the ISP with the COREX, the direct CO_2 emissions accounted for the largest proportion of the total CO_2 emissions. With the International Energy Agency factor, the direct CO_2 emissions accounted for 93.2%, 79.8%, and 97.9% of the total CO_2 emissions in the three routes, respectively. With the China Grid factor, the direct CO_2 emissions accounted for 88.5%, 66.0% and 96.5% of the total CO_2 emissions of the three routes. The net CO_2 emissions in the conventional ISP, the ISP with the TGR-OBF, and the ISP with the COREX increased from 1.94 t/t-steel, 1.73 t/t-steel, and 2.66 t/t-steel (International Energy Agency factor) to 2.05 t/t-steel, 2.11 t/t-steel, and 2.70 t/t-steel (China Grid factor), respectively. The increases were 5.7%, 22%, and 3.8%, respectively. This is because the indirect CO_2 emissions can be influenced by the CO_2 emissions factor. Furthermore, the more the electricity purchased by an ISP, the greater the impact of the CO_2 emissions factor. Therefore, if the International Energy Agency factor was used, the net CO_2 emissions of the ISP with the TGR-OBF was the lowest, followed by the conventional ISP, and the ISP with the COREX. However, if the China Grid factor was used, the net CO_2 emissions of the ISP with the TGR-OBF was not the lowest. That is to say, the net CO_2 emissions of the ISP with the TGR-OBF rely heavily on the electricity CO_2 emissions factor. When compared with the conventional ISP and the

ISP with the COREX, the ISP with the TGR-OBF had the lowest direct CO_2 emissions and the highest indirect CO_2 emissions. This is due to its lowest coal consumption and highest electricity consumption when compared with the other routes. The ISP with the COREX had the highest net CO_2 emissions for consuming a large amount of coal, which was 37.1% and 53.8% higher (International Energy Agency factor) as well as 31.7% and 28.0% higher (China Grid factor) than that of the conventional ISP and the ISP with the TGR-OBF, respectively.
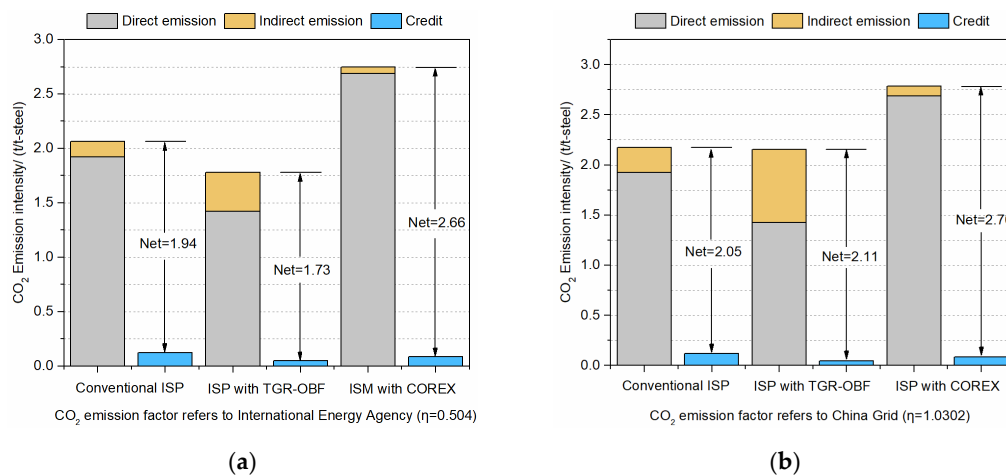
Figure 10. The CO_2 emissions intensity in the conventional ISP, the ISP with the TGR-OBF, and the ISP with the COREX with the CO_2 emissions factor referring to the world average (**a**) or North China Grid (**b**).

4. Conclusions

Based on two static process models, the material flows of the TGR-OBF and COREX ironmaking processes were investigated. Combining the operating data of the Jingtang steel plant, three steel production routes of the ISP with the BF, TGR-OBF, and COREX were analyzed comparatively on the material flows, metallurgical gas generation and consumption, electricity consumption and generation, comprehensive energy consumption, and CO_2 emissions. Compared with the conventional ISP, coking coal consumption in the ISP with the TGR-OBF and the ISP with the COREX were reduced by 39.7% and 100%. The coal consumption in the ISP with the TGR-OBF and the ISP with the COREX increased by 23.6% and 535.2%. Among the three routes, the electricity purchased for the ISP with the TGR-OBF was the highest with 710.1 kWh/t-steel and the ISP with the COREX was the lowest with 77.3 kWh/t-steel. The energy consumption of the ISP with the TGR-OBF was 16% and 16.5% lower than that of the conventional ISP and the ISP with the COREX, respectively. The energy consumption of the ISP with the COREX was the highest with 16.96 GJ/t-steel. The ISP with the COREX had the highest net CO_2 emissions, which was 37.1% and 53.8% higher (International Energy Agency factor) as well as 31.7% and 28.0% higher (China Grid factor) than that of the conventional ISP and the ISP with TGR-OBF. Although the ISP with COREX had no advantages in energy consumption and carbon emissions, it had the least purchased electricity and coke consumption. In addition, the ISP with TGR-OBF had the lowest energy consumption. Therefore, the ISP with the COREX is suitable for the areas with high electricity prices and where the coke is not available. Moreover, the ISP with the TGR-OBF should be carefully considered when the CCS technology is not applied.

Nomenclature

m	mass of substance (kg)
e_i^{in}, e_i^{out}	the input and output energy substances (kg/t crude steel)
CE, CE_d, CE_i, CE_c	the net, direct, indirect, and credit of the CO_2 emissions (t/t crude steel)
C_{in}, C_p, C_{byp}	the amount of total carbon input to the system, the amount of carbon fixed in the product, the amount of carbon fixed in the byproduct (t/t crude steel)
h	Specific enthalpy of chemical reaction (kJ/kg)
H	enthalpy value (kJ)
K	equilibrium constant
OD	oxidation degree
p_i	energy conversion coefficient for substance i (GJ/kg)
q	sensible heat (kJ/kg)
R	basicity
T	temperature (K)
v	gas volume fraction
V	gas volume (m^3)
ω	mass fraction

References

1. World Steel Association. *World Steel in Figures 2018 Now Available*; World Steel Association: Brussels, Belgium, 2018.
2. Chen, W.; Yin, X.; Ma, D. A bottom-up analysis of China's iron and steel industrial energy consumption and CO_2 emissions. *Appl. Energy* **2014**, *136*, 1174–1183. [CrossRef]
3. Shen, X.; Chen, L.; Xia, S.; Xie, Z.; Qin, X. Burdening proportion and new energy-saving technologies analysis and optimization for iron and steel production system. *J. Cleaner Prod.* **2018**, *172*, 2153–2166. [CrossRef]
4. Smith, M.P. Blast furnace ironmaking—A view on future developments. *Procedia Eng.* **2017**, *174*, 19–28. [CrossRef]
5. Wenzel, W. Hochofenbetrieb mit gasformigen Hilfsreduktionsmitteln. Germany Patent 2030468, 1970.
6. Fink, F. Suspension smelting reduction—A new method of hot iron production. *Steel Times (UK)* **1996**, *224*, 398–399.
7. Lu, W.; Kumar, R.V. The feasibility of nitrogen free blast furnace operation. *ISS Trans.* **1984**, *5*, 25.
8. Ohno, Y.; Hotta, H.; Matsuura, M.; Mitsufuji, H.; Saito, H. Development of oxygen blast furnace process with preheating gas injection into upper shaft. *Tetsu-to-Hagané* **1989**, *75*, 1278–1285. [CrossRef]
9. Pukhov, A. Introduction of blast furnace technology involving injection of hot reducing gases. *Publ. Steel USSR* **1991**, *21*, 333–338.
10. Qin, M.; Gao, K.; Wang, G. Study on operation of blast furnace full oxygen blast. *Iron Steel* **1987**, *22*, 1–7. (In Chinese)
11. Danloy, G.; Berthelemot, A.; Grant, M.; Borlée, J.; Sert, D.; Van der Stel, J.; Jak, H.; Dimastromatteo, V.; Hallin, M.; Eklund, N.; et al. ULCOS-Pilot testing of the low-CO_2 blast furnace process at the experimental BF in Luleå. *Rev. Mét. Inter. J. Metall.* **2009**, *106*, 1–8. [CrossRef]
12. Yamaoka, H.; Kamei, Y. Theoretical study on an oxygen blast furnace using mathematical simulation model. *ISIJ inter.* **1992**, *32*, 701–708. [CrossRef]

13. Yamaoka, H.; Kamei, Y. Experimental study on an oxygen blast furnace process using a small test plant. *ISIJ Inter.* **1992**, *32*, 709–715. [CrossRef]

14. Babich, A.I.; Gudenau, H.W.; Mavrommatis, K.T.; Froehling, C.; Formoso, A.; Cores, A.; Garcia, L. Choice of technological regimes of a blast furnace operation with injection of hot reducing gases. *Revista De Metalurgia* **2002**, *38*, 288–305. [CrossRef]

15. Jin, P.; Jiang, Z.; Bao, C.; Lu, Y.; Zhang, J.; Zhang, X. Mathematical modeling of the energy consumption and carbon emission for the oxygen blast furnace with top. *Gas Steel Res. Int.* **2016**, *87*, 320–329. [CrossRef]

16. Mitra, T.; Helle, M.; Pettersson, F.; Saxén, H.; Chakraborti, N. Multiobjective optimization of top gas recycling conditions in the blast furnace by genetic algorithms. *Mater. Manuf. Processes* **2011**, *26*, 475–480. [CrossRef]

17. Liu, L.; Jiang, Z.; Zhang, X.; Lu, Y.; He, J.; Wang, J.; Zhang, X. Effects of top gas recycling on in-furnace status, productivity, and energy consumption of oxygen blast furnace. *Energy* **2018**, *163*, 144–150. [CrossRef]

18. Zhang, W.; Zhang, J.; Xue, Z. Exergy analyses of the oxygen blast furnace with top gas recycling process. *Energy* **2017**, *121*, 135–146. [CrossRef]

19. Zhu, K. Analysis of COREX process as a new ironmaking technology. *Fuel Energy Abstr.* **1995**, *4*, 284.

20. Guo, Z.C.; Fu, Z.X. Current situation of energy consumption and measures taken for energy saving in the iron and steel industry in China. *Energy* **2010**, *35*, 4356–4360. [CrossRef]

21. Eberle, A.; Siuka, D.; Bohm, C. New Corex C-3000 plant for Baosteel and status of the Corex technology. *Stahl Und Eisen* **2006**, *126*, 31–+.

22. Hasanbeigi, A.; Arens, M.; Price, L. Alternative emerging ironmaking technologies for energy-efficiency and carbon dioxide emissions reduction: A technical review. *Renew. Sustain. Energy Rev.* **2014**, *33*, 645–658. [CrossRef]

23. Zhan, W.; Wu, K.; He, Z.; Liu, Q.; Wu, X. Estimation of energy consumption in COREX process using a modified rist operating diagram. *J. Iron. Steel Res. Int.* **2015**, *22*, 1078–1084. [CrossRef]

24. Hu, C.; Han, X.; Li, Z.; Zhang, C. Comparison of CO_2 emission between COREX and blast furnace iron-making system. *J. Environ. Sci.* **2009**, *21*, S116–S120. [CrossRef]

25. She, X.; An, X.; Wang, J.; Xue, Q.; Kong, L. Numerical analysis of carbon saving potential in a top gas recycling oxygen blast furnace. *J. Iron. Steel Res. Int.* **2017**, *24*, 608–616. [CrossRef]

26. Hooey, L.; Tobiesen, A.; Johns, J.; Santos, S. Techno-economic study of an integrated steelworks equipped with oxygen blast furnace and CO_2 capture. *Energy Procedia* **2013**, *37*, 7139–7151. [CrossRef]

27. He, H.; Guan, H.; Zhu, X.; Lee, H. Assessment on the energy flow and carbon emissions of integrated steelmaking plants. *Energy Rep.* **2017**, *3*, 29–36. [CrossRef]

28. Jin, P.; Jiang, Z.; Bao, C.; Hao, S.; Zhang, X. The energy consumption and carbon emission of the integrated steel mill with oxygen blast furnace. *Resour. Conserv. Recycl.* **2017**, *117*, 58–65. [CrossRef]

29. Arasto, A.; Tsupari, E.; Kärki, J.; Lilja, J.; Sihvonen, M. Oxygen blast furnace with CO_2 capture and storage at an integrated steel mill—Part I: Technical concept analysis. *Int. J. Greenh. Gas Control* **2014**, *30*, 140–147. [CrossRef]

30. Tsupari, E.; Kärki, J.; Arasto, A.; Lilja, J.; Kinnunen, K.; Sihvonen, M. Oxygen blast furnace with CO2 capture and storage at an integrated steel mill—Part II: Economic feasibility in comparison with conventional blast furnace highlighting sensitivities. *Int. J. Greenhouse Gas Control* **2015**, *32*, 189–196. [CrossRef]

31. Jin, P. Feasibility Investigation on Oxygen Blast Furnace with Top Gas Recycling Based on Multi-427 Level Models. PhD Thesis, University of Science and Technology Beijing, Beijing, China, 2 November 2015.

32. Arasto, A.; Tsupari, E.; Kärki, J.; Pisilä, E.; Sorsamäki, L. Post-combustion capture of CO_2 at an integrated steel mill—Part I: Technical concept analysis. *Int. J. Greenhouse Gas Control* **2013**, *16*, 271–277. [CrossRef]

33. Liu, Z.; Grande, C.; Li, P.; Yu, J.; Eodrigues, A. Multi-bed vacuum pressureswing adsorption for carbon dioxide capture from flue gas. *Sep. Purif. Technol.* **2011**, *81*, 307–317. [CrossRef]

34. Standardization Administration of China. *General Principles for Calculation of the Comprehensive Energy Consumption*; Standardization Administration of China: Beijing, China, 2008.

35. World Resources Institute & World Business Council for Sustainable Development. *The Greenhouse Gas Protocol*; WRI: Washington, DC, USA, 2013.